Journal of Zhejiang University SCIENCE
ISSN 1009-3095
http://www.zju.edu.cn/jzus
E-mail: jzus@zju.edu.cn

Correlation of liquefaction resistance with shear wave velocity based on laboratory study using bender element*

ZHOU Yan-guo (周燕国)†, CHEN Yun-min (陈云敏), KE Han (柯 瀚)

(*Department of Civil Engineering, Zhejiang University, Hangzhou 310027, China*)

†E-mail: qzking@zju.edu.cn

Received July 22, 2004; revision accepted Feb. 3, 2005

Abstract: Recent studies using field case history data yielded new criteria for evaluating liquefaction potential in saturated granular deposits based on in situ, stress-corrected shear wave velocity. However, the conditions of relatively insufficient case histories and limited site conditions in this approach call for additional data to more reliably define liquefaction resistance as a function of shear wave velocity. In this study, a series of undrained cyclic triaxial tests were conducted on saturated sand with shear wave velocity V_s measured by bender element. By normalizing the data with respect to minimum void ratio, the test results, incorporated with previously published laboratory data, statistically revealed good correlation of cyclic shear strength with small-strain shear modulus for sandy soils, which is almost irrespective of soil types and confining pressures. The consequently determined cyclic resistance ratio, *CRR*, was found to be approximately proportional to V_s^4. Liquefaction resistance boundary curves were established by applying this relationship and compared to liquefaction criteria derived from seismic field measurements. Although in the range of V_{s1}>200 m/s the presented curves are moderately conservative, they are remarkably consistent with the published field performance criteria on the whole.

Key words: Liquefaction resistance, Shear wave velocity, Sand, Cyclic triaxial test, Laboratory correlation, Bender element
doi:10.1631/jzus.2005.A0805 **Document code:** A **CLC number:** TU411.8; TU435

INTRODUCTION

Evaluation of soil liquefaction resistance is an important aspect of geotechnical engineering practice, and several types of evaluating procedures have evolved over the last three decades. The well known "simplified procedure" originated by Seed and Idriss (1971) can be used to evaluate liquefaction resistance based on standard penetration test (SPT) blow counts. Over the years, the simplified procedure has been modified and updated with additional data, and has become the most commonly used way to assess the potential for granular soils to liquefy (Robertson and Wride, 1998; Harder, 1997). While liquefaction criteria based on SPT and CPT data are fairly well developed, penetration tests may be impractical, or unreliable at some sites.

The use of V_s as an index of liquefaction resistance is soundly based because both V_s and liquefaction resistance are similarly influenced by many of the same factors (e.g., void ratio, state of stress, stress history, and geologic age). The advantages of the shear wave velocity-based method were pointed out by many researchers (Andrus and Stokoe, 2000; Rauch *et al*., 2000), and this method can provide a promising alternative and supplementary means of liquefaction assessment. Over the past 20 years, numerous studies have been conducted to investigate the relationship between V_s and liquefaction resistance. Excellent reviews of these proposed V_s-based procedures were provided by Andrus *et al*.(1999) and Andrus and Stokoe (2000). However, this approach is

* Project supported by the National Natural Science Foundation of China (No. 10372089), and Department of Education of Zhejiang Province (No. 20010572), China

hindered by the relatively small number of case histories and the limited range of site conditions represented in the data catalog, and additional data are needed to more reliably define liquefaction resistance as a function of shear wave velocity (Andrus *et al*., 1999). Because of the advantages mentioned above, laboratory studies can be used thereby, in conjunction with the available field performance data, to broaden the applicability of liquefaction criteria based on V_s.

In this study, a series of stress-controlled undrained cyclic triaxial tests were conducted on saturated reconstituted sand specimens with shear wave velocity measured using bender element. Incorporated with previously published laboratory data in the literature, a good relationship between the liquefaction resistance (represented by cyclic shear strength, *CSS*) and small-strain shear modulus (or the corresponding shear wave velocity) can be obtained from the test results. And the consequently determined cyclic resistance ratio, *CRR*, is found to be approximately proportional to V_s^4. Liquefaction resistance curves were established by applying this relationship and then compared with the field performance curves.

LABORATORY INVESTIGATION

Preliminary consideration

In all the abovementioned studies, it was well recognized that for a given type of soil, with other conditions (e.g., relative density) unchanged, the undrained cyclic triaxial strength (or CRR_{tx}) will keep constant despite the variation of confining pressure. In other words, for a soil liquefied in cyclic triaxial test at a given number of cycles, the imposed maximum cyclic shear stress in a load cycle, τ_d, is basically proportional to its effective confinement, σ_m', which could be expressed as

$$\left(\tau_d = \frac{\sigma_d}{2}\right) \propto \sigma_m' \tag{1}$$

in which σ_d is the cyclic deviator stress; and σ_m' is

$$\sigma_m' = \frac{1+2K_0}{3}\sigma_v' \tag{2}$$

where σ_v' is vertical effective confining pressure and K_0 is the earth pressure coefficient at rest. Thus the cyclic resistance ratio for cyclic triaxial tests, CRR_{tx}, can be defined as the cyclic stress ratio causing liquefaction in a given number of loading cycles corresponding to an earthquake magnitude M_w, when the double-amplitude axial strain reaches 5% (Ishihara, 1996).

In general, small-strain shear modulus, G_{max}, is given by (Hardin and Richart, 1963)

$$G_{max} = AF(e)(\sigma_m')^n \tag{3}$$

where A is an empirical constant reflecting soil fabric formed through various stress and strain histories; n is an empirically determined exponent, approximately equal to 1/2; σ_m' is mean effective confining pressure; e is void ratio and $F(e)$ is void ratio function, $F(e)=(2.97-e)^2/(1+e)$ for angular grain sands, and for round grain sands $F(e)=(2.17-e)^2/(1+e)$.

Eq.(3) implies the following empirical relation given by

$$G_{max} \propto (\sigma_m')^{1/2} \tag{4}$$

Combining Eq.(1) and Eq.(4) yields

$$\left(\tau_d = \frac{\sigma_d}{2}\right) \propto G_{max}^2 \tag{5}$$

Eq.(5) indicates that if the possible relationship between cyclic shear strength and the small-strain shear modulus could be established in laboratory, the corresponding cyclic resistance ratio, CRR_{tx}, can be easily correlated to the measured shear wave velocity. Since the conversion from the laboratory-derived indexes such as CRR_{tx} to field K_0 conditions is well studied and defined (Tokimatsu and Uchida, 1990; Andrus and Stokoe, 2000), the laboratory study on the correlation of liquefaction resistance with shear wave velocity will positively enhance the applicability of liquefaction criteria based on V_s.

Test material and apparatus

The tested soil was Fuzhou Sand, a kind of angular grained sand with D_{10}=0.13 mm and the coefficient of uniformity U_c=3.0. The specific gravity of the test material was 2.65. Minimum and maximum void ratios were 0.43 and 0.79, respectively.

To measure the small-strain shear modulus of soils before undrained cyclic loading, a piezoceramic bender elements system was established based on Model HX-100 multi-use triaxial apparatus, allowing low-strain acoustic wave velocities to be determined in the same specimen which will subsequently be loaded to failure at large strain. The test system and its application were discussed detailedly by Huang *et al*. (2001) and Zhou *et al*.(2005a; 2005b).

Bender elements served as versatile transducers for small-strain testing of wet or dry soils in a variety of cells and loading conditions (Shirley and Hampton, 1978; de Alba *et al*., 1984; Dyvik and Madshus, 1985; Thomann and Hryciw, 1990; Viggiani and Atkinson, 1995). The shear wave velocity V_s in the specimen can be calculated from the wave travel time t and the known separation L between the bender elements as $V_s=L/t$. For a known material density ρ, the small strain shear modulus can thus be calculated by

$$G_{max} = \rho V_s^2 \tag{6}$$

Specimen preparation and test procedures

Specimens with three different relative densities (45%, 60%, and 75%) were prepared by the saturated-tamping method, which consists of pouring sand into a specimen mold filled with de-aired water in five equal layers and tamping it to the desired height. The water level was kept above the soil surface at all times, and the sand was added slowly to minimize the segregation of fines. The specimen was 39.1 mm in diameter and 80 mm in height.

Each specimen was consolidated isotropically for 4 h at a given confinement and the shear wave velocity was measured for G_{max} before undrained cyclic loading. Specimen deformations during consolidation were measured and used to determine the final specimen density. Then it was subjected to uniform amplitude cyclic loading until liquefaction occurred at a frequency of 1 Hz.

TEST RESULTS AND ANALYSES

Relationship between *CSS* and G_{max}

The shear wave velocities and consolidated void ratio at different confining pressures, 50, 100, and 200 kPa for three relative densities were measured, and the corresponding data on cyclic stress ratio versus number of cycles to cause *DA*=5% was recorded. Then the data on cyclic shear strength with the corresponding shear modulus can be derived, which are plotted in Fig.1, together with those from Hangzhou Sand tested previously by Ke and Chen (2000). Although the data in Fig.1 are relatively scattered, they exhibit a highly linear trend if the plot has its longitudinal coordinate converted to $G_{max}/F(e_{min})$ and its vertical coordinate to $(\tau_{15})^{0.5}$ (Fig.2).

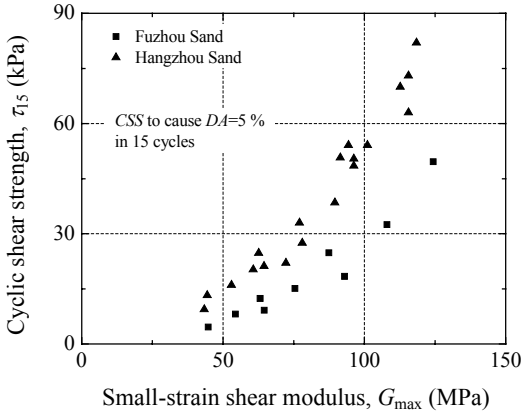

Fig.1 Original data on cyclic shear strength τ_{15} with G_{max}

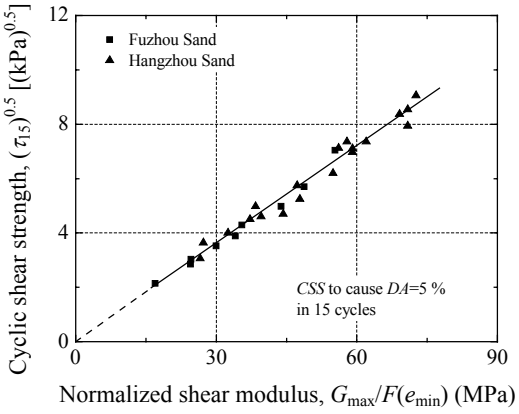

Fig.2 Data on $(\tau_{15})^{0.5}$ with corrected $G_{max}/F(e_{min})$

To further verify this interesting finding, intensive investigation on correlated researches was conducted and the previously published data on cyclic shear strength with the corresponding small-strain shear modulus of sandy soils were collected (Tokimatsu and Uchida, 1990; Chen and Liao, 1999; Huang *et al*., 2004), and their physical properties and grain characteristics are given in Table 1. All the collected data, together with the presented data in this study, were treated in the same manner as done in Figs.1 and 2, and plotted in Figs.3 and 4, respectively.

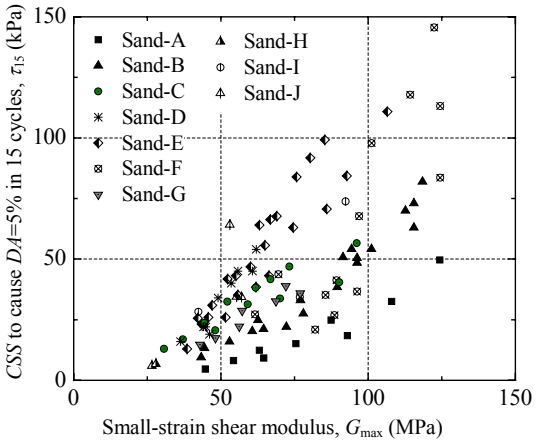

Fig.3 Data on τ_{15} with G_{max} for collected sands

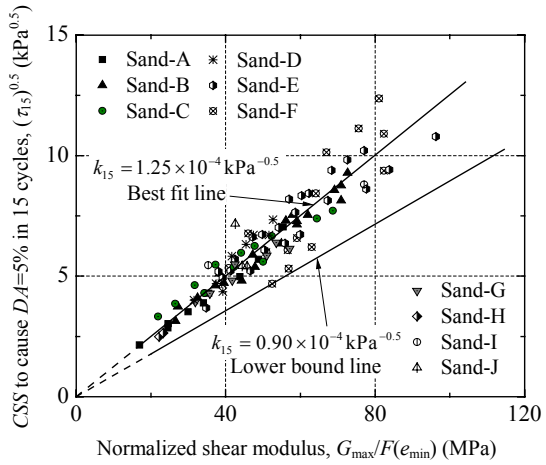

Fig.4 Data on $(\tau_{15})^{0.5}$ with $G_{max}/F(e_{min})$ for collected sands

Compared with those in Fig.1, data in Fig.3 show more evident diversity because of the different soil types and test conditions; while in Fig.4 with converted coordinates, they statistically reproduce the linear correlation of $(\tau_{15})^{0.5}$ with $G_{max}/F(e_{min})$, despite the material and confining pressure dependence.

If the slope of the fitting curves in Fig.4 is defined as k_{15}, the cyclic shear strength in 15 loading cycles, τ_{15}, could be expressed by

$$\tau_{15} = k_{15}^2 G_{max}^2 / F^2(e_{min}) \tag{7}$$

Thus, for more general conditions with cyclic number N, the corresponding cyclic shear strength, τ_N, can be readily extrapolated and expressed as

$$\tau_N = k_N^2 G_{max}^2 / F^2(e_{min}) \tag{8}$$

where k_N is the corresponding slope value. The experimental studies have confirmed the relationship between cyclic shear strength and small-strain shear modulus of soils assumed in Eq.(5).

Derivation of the correlation of *CRR* and V_s from laboratory results

Substituting Eq.(6) into Eq.(8), one may obtain the cyclic resistance ratio measured in laboratory triaxial tests given by

$$CRR_{tx} = \frac{\tau_N}{\sigma'_m} = \frac{k_N^2 \rho^2 V_s^4}{F^2(e_{min})\sigma'_m} \tag{9}$$

Eq.(9) explicitly reveals the laboratory correlation of cyclic resistance ratio with measured shear wave velocity, that is, CRR_{tx} changes proportionally with V_s^4.

However, in applying the results from cyclic traxial tests to in-situ conditions, the CRR_{tx} should be adjusted to account for the laboratory test conditions

Table 1 Physical properties and grain characteristics of studied sands

Sand type	Label	G_s	D_{10} (mm)	U_c	FC (%)	e_{min}	e_{max}	σ'_m (kPa)
Fuzhou Sand	Sand-A	2.65	0.13	3.0	0.0	0.43	0.79	50,100,200
Hangzhou Sand	Sand-B	2.69	0.12	2.4	1.0	0.57	1.23	50,100,200
Taiwan Sand	Sand-C	2.70	0.08	3.5	5/10/15	0.59	1.15	98,196
Mailiao Sand	Sand-D	2.69	0.09	2.4	0/15/30	0.65	–	100
Niigata Sand	Sand-E	2.69	0.18	1.7	0.2	0.78	1.21	49,98,196
Toyoura Sand	Sand-F	2.64	0.16	1.4	0.0	0.61	0.99	49,98,196
Meike Sand	Sand-G	2.73	0.16	1.6	0.2	0.67	1.07	50,65,75,80,85
Silica Sand	Sand-H	2.68	0.16	1.8	0.0	0.73	1.17	36
Makuhari Sand	Sand-I	2.71	0.10	2.1	5.4	0.73	1.18	47,120
Ohgishima Sand	Sand-J	2.72	0.12	2.1	4.0	0.78	1.28	77,83,90

which are different from those in the field. In an approximate manner, this correction can be made using the following equation (Seed, 1979):

$$CRR = r_c \frac{1+2K_0}{3} CRR_{tx} \tag{10}$$

where r_c is a constant accounting for the effect of multidirectional shaking (value of 0.9~1.0).

The laboratory measured velocity V_s at the right-hand part of Eq.(9) also requires modification for in-situ application. Using the procedure suggested by Andrus *et al*.(1999) and Eq.(2), one obtains the following relationship for converting the laboratory measured V_s to overburden stress-corrected V_{s1}:

$$V_{s1} = V_s \left(\frac{P_a}{\sigma'_v}\right)^{\frac{1}{4}} = V_s \left(\frac{P_a}{\sigma'_m}\right)^{\frac{1}{4}} \left(\frac{1+2K_0}{3}\right)^{\frac{1}{4}} \tag{11}$$

where P_a is a reference overburden stress (Robertson *et al*., 1992), and equals to 100 kPa.

Substituting Eqs.(10) and (11) into Eq.(9) yields the following expression for the equivalent field *CRR* in terms of V_{s1} and other factors:

$$CRR = r_c \frac{k_N^2 \rho^2 V_{s1}^4}{F^2(e_{min}) P_a} \tag{12}$$

It is interesting that although the earth pressure coefficient at rest K_0 is involved in Eqs.(10) and (11), its effect on the resulting expression for the relationship between equivalent field *CRR* and V_{s1} converted from laboratory results is almost cancelled out. Tokimatsu and Uchida (1990) also mentioned this issue, and suggested that any value between 0.5 and 1.0 might be assumed for practical purposes.

Eq.(12) can be directly used to evaluate the liquefaction resistance of in situ ground with the known soil property values such as mass density, ρ, minimum void ratio, e_{min}, and the slope of fitting line summarized from laboratory tests, k_N. The determination of these values is discussed below.

Based upon the relationship of k_N-*CRR* implied in Eq.(12), for magnitudes other than 7.5, the k_N in Eq.(12) could be obtained as:

$$k_N = k_{15}\sqrt{MSF} = k_{15}\left(\frac{M_w}{7.5}\right)^{n/2} \tag{13}$$

where *MSF* is magnitude scaling factor to account for the effect of earthquake magnitude (M_w), and equals 1.0 for earthquakes with a magnitude of 7.5; n is exponent with lower bound −2.56 recommended by the 1996 NCEER workshop and upper bound −3.3 (Andrus and Stokoe, 1997) for earthquakes with magnitudes≤7.5.

In Fig.4 the slope values could be directly calculated as k_{15}=1.25×10^{-4} kPa$^{-1/2}$ for the "best-fit" line and k_{15}=0.90×10^{-4} kPa$^{-1/2}$ for the "lower bound" one. And k_N corresponding to other magnitudes could be easily determined from Eq.(13) with the typical correlation between the number of cycles and the earthquake magnitude (Seed *et al*., 1985), which are shown in Table 2.

Table 2 Values of k_N for different M_w (×10^{-4} kPa$^{-1/2}$)

M_w	Cycle number	n=−2.56		n=−3.3	
		Best fit	Lower bound	Best fit	Lower bound
5–1/4	2~3	1.97	1.42	2.25	1.62
6	5	1.66	1.20	1.81	1.30
6–3/4	10	1.43	1.03	1.49	1.07
7–1/2	15	1.25	0.90	1.25	0.90
8–1/2	26	1.06	0.77	1.02	0.73

If the minimum void ratio is unknown, it may be evaluated from the empirical relationship between maximum and minimum void ratios and fines content presented by Sakai and Yasuda (1977). Tokimatsu and Uchida (1990) recommended the average values of the minimum void ratio as the first approximation, which is 0.65 for sands with fines content less than 20%, 0.75 for silty sands, and 0.95 for sandy silt.

COMPARISON WITH FIELD CORRELATION

Detailed comparison between previous curves and the present one

As mentioned above, if the values of laboratory obtained k_N and other easily determined soil properties are given, the in-situ *CRR* can be directly correlated to the overburden stress-corrected shear wave

velocity V_{s1} based on Eq.(12). Thus it is convenient to compare the boundary curves calculated from Eq.(12) with those developed by Andrus and Stokoe (2000) from field performance data.

In the case of 15 loading cycles corresponding to earthquakes with magnitude of 7.5, the values in Eq.(12) may be adopted as follows: k_{15}=1.25×10^{-4} kPa$^{-1/2}$ (best-fit) and 9.00×10^{-5} kPa$^{-1/2}$ (lower bound); ρ=1.90 g/cm^3 (recommended by Andrus *et al*., 1999); e_{min}=0.65; P_a=100 kPa. The calculated results are plotted in Fig.5 together with field performance data with FC≤5%, in consideration of the fact that most of the laboratory data studied herein were from samples with fines content less than 5%.

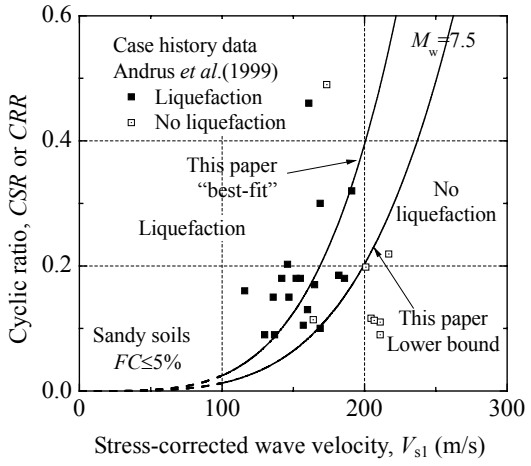

Fig.5 Curves by Eq.(12) for *CRR* from V_{s1} and case history data for sands with *FC*≤5% (Andrus *et al*., 1999)

As can be seen in Fig.5, the boundary curves calculated from Eq.(12) with lower bound value of k_{15} can separate quite well the liquefiable from the non-liquefiable field conditions, while the one with "best fit" k_{15} value lies in the liquefied data points and tends to separate them evenly. The characteristics of the two curves echo those presented by Andrus *et al*. (1999), which were converted from the laboratory test results by Tokimatsu and Uchida (1990) (Fig.6). Compared with the corresponding boundary curve recommended by Andrus and Stokoe (2000), the laboratory-test-based boundary curves presented either by the present authors or by Tokimatsu and Uchida (1990) strongly imply that, the curve of "lower bound" slope is the most probable one appropriate for evaluating the liquefaction resistance of soils while the "best fit" curve is mere the median curve of liquefied case history data, since it corresponds to the median line summarized from various liquefied laboratory data.

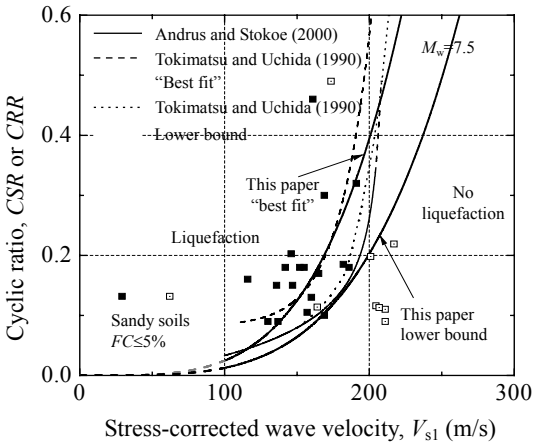

Fig.6 Curves by Eq.(12) for *CRR* from V_{s1} together with those recommended by Andrus and Stokoe (2000)

Argument for the superiority of the present laboratory correlation

It is interesting to note that even for the case history data of sandy soils with average FC>5%, the presented curve also performs well (Fig.7). Also notice that, in Fig.7, the Andrus and Stokoe recommended curve is sensitive to the precision of the measured shear wave velocity. For values of V_{s1} in the range of 190 to 220 m/s, where the curve turns sharply upward, small changes in V_{s1} correspond to large changes in *CRR*. While the "lower bound" curve proposed in this paper behaves in a relatively slower

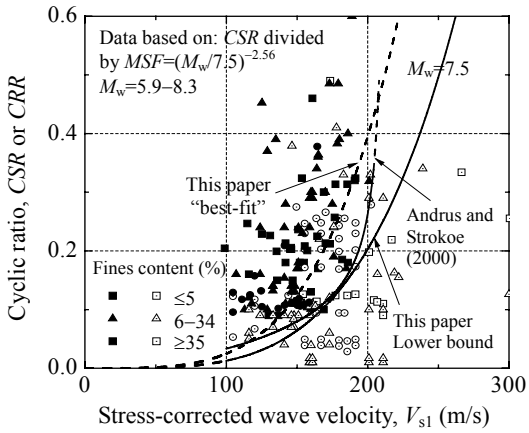

Fig.7 Curves by Eq.(12) with that recommended by Andrus and Stokoe (2000) along with case history data

way. The curve from Andrus and Stokoe was established essentially by applying a modified relationship between shear wave velocity and cyclic stress ratio for constant average cyclic shear strain, and adjusted to be validated through the case history data, so it is consequently limited by the case history database and should keep open to new field performance data, especially those from denser soil deposits shaken by stronger ground motions (e.g., the dashed Andrus curve above *CRR* of 0.35 indicates that field performance data are limited).

To bolster the abovementioned arguments, the Chi-Chi strong earthquake history data (M_w=7.6, Taiwan, 1999) are added. Following the procedure proposed by Andrus *et al*.(1999), seven liquefied site performance data are adjusted and plotted together with the previous case history data (Fig.8). It is noticeable that two of the Chi-Chi data fall below the Andrus and Stokoe proposed curve. However, the curves presented by this paper perform remarkably well: the "lower bound" curve separates the liquefied data correctly and the "best fit" one lies almost in the middle of the seven data points. Thus, the *CRR*-V_{s1} curves proposed in this paper are recommended because they were based on abundant laboratory data and checked by the largest, most correct case history data set and procedures (Andrus *et al*., 1999). Admittedly, due to the relatively small number of laboratory data with lower V_{s1}<100 m/s (the corresponding value is in the range of about 110 to 250 m/s), additional data are needed to more reliably define the

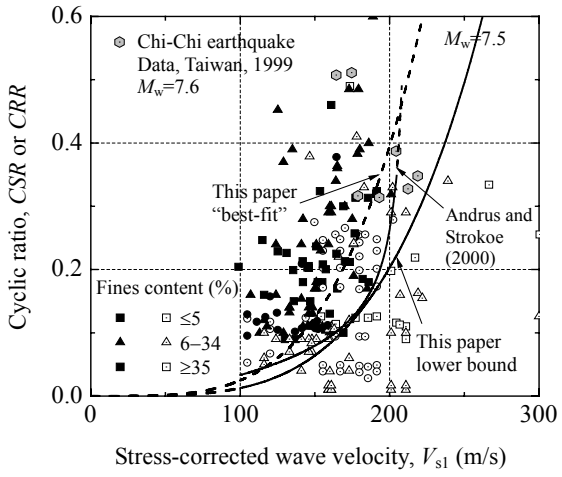

Fig.8 Performance comparison between the curves by Eq.(12) and that by Andrus and Stokoe (2000) with Chi-Chi strong earthquake data

correlation of liquefaction resistance with the shear wave velocity derived herein. In other words, the summarized correlation in this paper is also open and developable.

SUMMARY AND CONCLUSIONS

Laboratory data relating liquefaction resistance to shear wave velocity V_s were obtained, by conducting undrained cyclic triaxial tests on saturated sand. The test results, incorporated with previously published laboratory data in the literature, revealed good correlation of cyclic shear strength with small-strain shear modulus for sandy soils. Based on this relationship, liquefaction resistance boundary curves were established and compared to liquefaction criteria derived from seismic field measurements. There was a good agreement between the laboratory test data and the field performance criteria. Recent strong earthquake data further validated the effectiveness and reliability of this laboratory correlation.

This study demonstrates the possible link between field and laboratory measurements of shear wave velocities. This link creates the opportunity to extend this approach to study other materials, such as silty sands and gravelly soils, and to study the influence of other parameters, such as high confining pressure, where little to no field performance data are available.

Meanwhile, in consideration of the complexity of liquefaction assessment, this laboratory correlation should be used cautiously and with engineering judgment when applying it to sites where conditions are different from those presented here, especially for those sites subjected to stronger seismic motions or with very low shear wave velocities.

ACKNOWLEDGEMENTS

The authors would like to thank the students at Zhejiang University, Miss Ma Yanhong, Mr. Lin Weian and Mr. Yang Zhi, for their kind cooperation in conducting part of the laboratory tests in this study.

References

Andrus, R.D., Stokoe, K.H.II, 1997. Liquefaction Resistance

Based on Shear Wave Velocity. Proc. NCEER Workshop on Evaluation of Liquefaction Resistance of Soils, Tech. Rep. NCEER-97-0022, National Center for Earthquake Engineering Research, Buffalo, p.89-128.

Andrus, R.D., Stokoe, K.H.II, 2000. Liquefaction resistance of soils from shear-wave velocity. *Journal of Geotechnical and Geoenvironmental Engineering*, *ASCE*, **126**(11): 1015-1025.

Andrus, R.D., Stokoe, K.H.II, Chung, R.M., 1999. Draft Guidelines for Evaluating Liquefaction Resistance Using Shear Wave Velocity Measurements and Simplified Procedures. NISTIR 6277, National Institute of Standards and Technology, Gaithersburg, MD.

Chen, Y.C., Liao, T.S., 1999. Dynamic Properties and State Parameter of Sand. Proceedings of the International Offshore and Polar Engineering Conference, **1**:529-535.

de Alba, P., Baldwin, K., Janoo, V., Roe, G., Celikkol, B., 1984. Elastic-wave velocities and liquefaction potential. *Geotechnical Testing Journal*, *ASTM*, **7**(2):77-87.

Dyvik, R., Madshus, C., 1985. Laboratory Measurement of G_{max} Using Bender Elements. Proceedings of ASCE Annual Convention: Advances in the Art of Testing Soils under Cyclic Conditions, Detroit.

Harder, L.F.Jr., 1997. Application of the Becker Penetration Test for Evaluating the Liquefaction Potential of Gravelly Soils. Proc. NCEER Workshop on Evaluation of Liquefaction Resistance of Soils, National Center for Engineering Research, Buffalo, p.129-148.

Hardin, B.O., Richart, F.E.Jr., 1963. Elastic wave velocities in granular soils. *Journal of the Soil Mechanics and Foundations Division*, *ASCE*, **89**(1):33-65.

Huang, B., Yin, J.H., Chen, Y.M., Wu, S.M., 2001. Measurements of elastic shear modulus G_{max} using piezoceramic bender elements. *Journal of Vibration Engineering*, **14**(2):155-160 (in Chinese).

Huang, Y.T., Huang, A.B., Kuo, Y.C., Tsai, M.D., 2004. A laboratory study on the undrained strength of a silty sand from Central Western Taiwan. *Soil Dynamics and Earthquake Engineering*, **24**:733-743.

Ishihara, K., 1996. Soil Behavior in Earthquake Geotechnics. Oxford Univ. Press, New York.

Ke, H., Chen, Y.M., 2000. An improved method for evaluating liquefaction potential by the velocity of shear-waves. *Acta Seismologica Sinica*, **22**(6):637-644.

Rauch, A.F., Duffy, M., Stokoe, K.H.II, 2000. Laboratory correlation of liquefaction resistance with shear wave velocity. *Geotechnical Special Publication*, *ASCE*, **110**:66-80.

Robertson, P.K., Wride, C.E., 1998. Evaluating cyclic liquefaction potential using the cone penetration test. *Canadian Geotechnical Journal*, **35**(3):442-459.

Robertson, P.K., Woeller, D.J., Finn, W.D.L., 1992. Seismic cone penetration test for evaluating liquefaction potential under cyclic loading. *Canadian Geotechnical Journal*, **29**:686-695.

Sakai, Y., Yasuda, S., 1977. Liquefaction Characteristics of Undisturbed Sandy Soils. Proc. 12th Annual Meeting JSSMFE, p.389-392 (in Japanese).

Seed, H.B., 1979. Soil liquefaction and cyclic mobility for level ground during earthquakes. *Journal of Geotechnical Engineering Division*, *ASCE*, **105**(2):201-255.

Seed, H.B., Idriss, I.M., 1971. Simplified procedure for evaluating soil liquefaction potential. *Journal of the Soil Mechanics and Foundation Division*, *ASCE*, **97**(9): 1249-1273.

Seed, H.B., Tokimatsu, K., Harder, L.F., Chung, R.M., 1985. The influence of SPT procedures in soil liquefaction resistance evaluations. *Journal of Geotechnical Engineering*, *ASCE*, **111**(12):1425-1445.

Shirley, D.J., Hampton, L.D., 1978. Shear wave measurements in laboratory sediments. *Journal of the Acoustical Society of America*, **63**(2):607-613.

Thomann, T.G., Hryciw, R.D., 1990. Laboratory measurement of small strain shear modulus under K_0 conditions. *Geotechnical Testing Journal*, *ASTM*, **13**(2):97-105.

Tokimatsu, K., Uchida, A., 1990. Correlation between liquefaction resistance and shear wave velocity. *Soils and Foundations*, *JSSMFE*, **30**(2):33-42.

Viggiani, G., Atkinson, J.H., 1995. The interpretation of the bender element tests. *Geotechnique*, **45**(1):149-154.

Zhou, Y.G., Chen, Y.M., Huang, B., 2005a. Experimental study of seismic cyclic loading effects on small strain shear modulus of saturated sands. *Journal of Zhejiang University SCIENCE*, **6A**(3):229-236.

Zhou, Y.G., Chen, Y.M., Ke, H., 2005b. Improvement on simplified procedure for liquefaction potential evaluation of sands by shear wave velocity. *Chinese Journal of Rock Mechanics and Engineering*, in Press (in Chinese).